


# Integrin alpha V beta 3 targeted dendrimer-rapamycin conjugate reduces fibroblast-mediated prostate tumor progression and metastasis

Elliott E. Hill<sup>1</sup> | Jin Koo Kim<sup>1,2,3</sup>  | Younghun Jung<sup>4</sup> | Chris K. Neeley<sup>5</sup> |  
Kenneth J. Pienta<sup>5</sup> | Russell S. Taichman<sup>4</sup> | Jacques E. Nor<sup>6</sup> |  
James R. Baker Jr<sup>7</sup> | Paul H. Krebsbach<sup>1,2,3</sup>

<sup>1</sup> Department of Biologic and Materials Sciences, University of Michigan School of Dentistry, Ann Arbor, Michigan

<sup>2</sup> Biointerfaces Institute, University of Michigan, Ann Arbor, Michigan

<sup>3</sup> Section of Periodontics, University of California, Los Angeles School of Dentistry, Los Angeles, California

<sup>4</sup> Department of Periodontics and Oral Medicine, University of Michigan School of Dentistry, Ann Arbor, Michigan

<sup>5</sup> Department of Urology, The James Buchanan Brady Urological Institute, Johns Hopkins School of Medicine, Baltimore, Maryland

<sup>6</sup> Department of Cariology, Restorative Sciences and Endodontics, University of Michigan School of Dentistry, Ann Arbor, Michigan

<sup>7</sup> Department of Internal Medicine, Pathology and Nanotechnology, University of Michigan, Ann Arbor, Michigan

## Correspondence

Paul H. Krebsbach, Section of Periodontics,  
University of California, Los Angeles  
School of Dentistry, Los Angeles, CA.  
Email: pkrebsbach@dentistry.ucla.edu

## Funding information

Department of Defense, Grant numbers:  
W81XW-15-1-0413, W81XWH-14-1-  
0403; National Cancer Institute,  
Grant numbers: CA093900, CA163124;  
Prostate Cancer Foundation

## Abstract

Therapeutic strategies targeting both cancer cells and associated cells in the tumor microenvironment offer significant promise in cancer therapy. We previously reported that generation 5 (G5) dendrimers conjugated with cyclic-RGD peptides target cells expressing integrin alpha V beta 3. In this study, we report a novel dendrimer conjugate modified to deliver the mammalian target of rapamycin (mTOR) inhibitor, rapamycin. In vitro analyses demonstrated that this drug conjugate, G5-FI-RGD-rapamycin, binds to prostate cancer (PCa) cells and fibroblasts to inhibit mTOR signaling and VEGF expression. In addition, G5-FI-RGD-rapamycin inhibits mTOR signaling in cancer cells more efficiently under proinflammatory conditions compared to free rapamycin. In vivo studies established that G5-FI-RGD-rapamycin significantly inhibits fibroblast-mediated PCa progression and metastasis. Thus, our results suggest the potential of new rapamycin-conjugated multifunctional nanoparticles for PCa therapy.

## KEYWORDS

dendrimer, fibroblast, integrin, metastasis, mTOR, prostate cancer, rapamycin, VEGF

## 1 | INTRODUCTION

In the progression of prostate cancer, metastasis often represents a fatal step, with 90% of deaths resulting from

metastases rather than from the primary tumor.<sup>1,2</sup> This finding has generated great interest in developing targeted cancer therapeutics. Effective therapies would target both the metastatic cells and cells of the microenvironment that permit their survival.<sup>3–7</sup> Angiogenesis is an essential process in tumor cell growth and survival, and the correlation between

Elliott E. Hill and Jin Koo Kim contributed equally to this work.

neovascularization, micro-vessel density, and metastatic carcinoma<sup>8,9</sup> has been confirmed as an important parameter in tumor progression.<sup>10,11</sup> Several studies demonstrate that growth factors in the tumor microenvironment and the local host tissues are active participants in this process.<sup>12,13</sup> One such growth factor, vascular endothelial growth factor (VEGF), is known to enhance the tumor angiogenic potential and has emerged as a target for anticancer therapy with several drugs currently in clinical trials.<sup>14,15</sup> Taken together, these findings have led to an intense interest in identifying innovative methods to modulate both the source and the impact of these angiogenic factors on tumor progression.<sup>10,11,14,16,17</sup>

Macrophages, infiltrating eosinophils, and fibroblasts are implicated in tumor progression.<sup>18–21</sup> More recently, stromal fibroblasts, the most abundant cell type in the stroma of carcinomas, have been identified as a source of VEGF and other factors that promote an angiogenic response to neoplasms.<sup>3,16,19,22</sup> Proliferating fibroblasts, enhanced capillary density, and deposition of type-1 collagen and fibrin are hallmarks of a tissue stroma response to tumor progression and metastasis.<sup>11,23,24</sup> Recent studies illustrate that these changes are, in part, regulated by integrin-fibroblast interactions.<sup>25</sup> Yet these fibroblasts have, until recently, been largely overlooked as targets in cancer therapy.

The mammalian target of rapamycin (mTOR) is a serine/threonine protein kinase that participates in the formation of two distinct signaling complexes; mTOR complex 1 (mTORC1), containing the regulatory-associated protein of mTOR (Raptor), and mTOR complex 2 (mTORC2), containing the rapamycin-insensitive companion of mTOR (Rictor). mTORC1 phosphorylates ribosomal S6 Kinase (S6K) and activated S6K phosphorylates ribosomal protein S6 (rpS6), stimulating protein synthesis, cell growth, and cell proliferation. In contrast, mTORC2 phosphorylates Akt and PKC $\alpha$ , promoting cell survival and cytoskeleton reorganization. Rapamycin, a specific inhibitor of mTOR, directly binds to mTORC1 and inhibits its activity. However, mTORC2 is insensitive to rapamycin, although prolonged treatment can inhibit mTORC2 in many cell types.<sup>26</sup>

Integrins play a key role in cell adhesion to RGD motifs within proteins of the extracellular matrix (ECM), triggering signal transduction mechanisms involved in stem cell self-renewal,<sup>27,28</sup> cell proliferation and survival,<sup>29</sup> and tumor metastasis.<sup>30</sup> We previously reported that generation 5 dendrimers can be conjugated with cyclic-RGD peptides that target and bind with specificity to cells that express high levels of the receptors for integrin  $\alpha$  V  $\beta$  3.<sup>31,32</sup> Here, we report the synthesis of a novel dendrimer conjugate with rapamycin, G5-FI-RGD-rapamycin. Furthermore, we report that G5-FI-RGD-rapamycin binds to prostate cancer cells as well as the fibroblasts that support them to suppress tumor progression. We also demonstrate that G5-FI-RGD-rapamycin blocks the mTOR

signaling pathway that modulates VEGF expression and subsequently impedes metastatic tumor progression.

## 2 | MATERIALS AND METHODS

### 2.1 | Dendrimer synthesis

Commercially available generation 5 (G5) poly amido amine (PAMAM) dendrimer (Dendritech, Midland, MI) was prepared and analyzed at the Michigan Nanotechnology Institute of Medicine and Biological Sciences as previously described. Briefly, G5 amine terminated dendrimer was partially neutralized via acetylation (0.01 mmol G5 amine dendrimer and 0.085 mmol triethyl amine/0.074 mmol acetic anhydride). The reaction was run overnight in anhydrous MeOH at room temperature. Subsequently, the reaction mixture was purified via dialysis (10 000 MWCO) and the average number of acetyl groups (75) was determined via a <sup>1</sup>H NMR calibration curve. G5Ac (75) was further modified via 1:3 molar addition of fluorescein isothiocyanate (FI) in DMSO overnight. Free FI dye was removed by an elution column (G25 sephadex). An active ester was prepared by reacting G5Ac (75) with an excess of glutaric anhydride, repeating purification via dialysis then reacting the conjugate with an excess of 1-[3-(Dimethylamino)propyl]-3-ethylcarbodiimide methiodide (EDC) and again repeating dialysis. Finally, a commercially available  $\alpha$ V $\beta$ 3 specific cyclic arginine-glycine-aspartic acid (RGD) peptide (cRGDyK, Peptides International, Louisville, KY) was added in a 5:1 molar ratio to G5Ac (75)-FI ester and purification steps were repeated. The esterification steps were repeated, then commercially available rapamycin (Sigma-Aldrich, St. Louis, MO) was added in a 8:1 ratio to the G5Ac (75)-FI-RGD conjugate and the final compound (G5-FI-RGD-rapamycin) was purified via dialysis.

### 2.2 | Cell culture

Primary bone marrow-derived stromal fibroblasts were collected from human or mouse bone marrow.<sup>33,34</sup> Primary fibroblasts and cancer cell lines (PC3, C4-2B, MDA-MB-231, and HeLa; American Type Culture Collection) were grown in Dulbecco's modified Eagle's medium (DMEM, Invitrogen, Carlsbad, CA) supplemented with 10% FBS and 1% penicillin/streptomycin. Human dermal microvascular endothelial cells (HDMEC; Cambrex, Walkersville, MD) were cultured in endothelial growth medium-2 for microvascular cells (EGM2-MV; Cambrex).

### 2.3 | Flow cytometry

Human fibroblast cells were treated with 200 nM G5-FI-RGD-rapamycin for 6 h with/without pre-treatment with 1  $\mu$ M free RGD peptide. Cells were then disassociated from the culture dish by trypsinization, washed in PBS and

analyzed via flow cytometry for mean fluorescent intensity (Beckman Coulter, Fullerton, CA).

## 2.4 | Immunofluorescence

Approximately  $5 \times 10^5$  human fibroblasts were seeded onto six well culture dishes (Matek Corp., Ashland, MA) and cultured in 3 mL of medium for at least 24 h before the initiation of the experimental conditions. Samples were treated with G5-FI-RGD-rapamycin (200 nM) for 6 h with/without pre-treatment with 1  $\mu$ M free RGD peptide and examined for G5-conjugate uptake using a Carl Zeiss confocal microscope.

## 2.5 | Western blot analysis

Whole cell lysates were prepared from cells, separated on 10% SDS-polyacrylamide gel and transferred to PVDF membrane. The membranes were incubated with 5% milk for 1 h and incubated with primary antibodies overnight at 4°C. Primary antibodies used were as follows: VEGF (1:1000; Santa Cruz, Santa Cruz, CA), FGF-2 (1:1000; Santa Cruz), phospho-S6K1 (Thr389) (1:1000; Cell Signaling, Danvers, MA), S6K1 (1:1000; Cell Signaling), phospho-S6 (Ser 240/244) (1:4000; Cell Signaling), and S6 (1:4000; Cell Signaling). Blots were incubated with peroxidase-coupled secondary antibodies (Promega, Madison, WI) for 1 h, and protein expression was detected with SuperSignal West Pico Chemiluminescent Substrate (Thermo Scientific, Rockford, IL). Membranes were reprobated with anti-GAPDH antibody (Chemicon, Temecula, CA) to control for equal loading.

## 2.6 | ELISA

HDMEC and human or mouse fibroblasts were treated with 200 nM G5-FI-RGD-rapamycin for 24 h. Supernatants of cell cultures were collected and centrifuged to eliminate cell debris. VEGF expression was determined by a human VEGF Quantikine ELISA kit (R&D systems, Minneapolis, MN) following the manufacturer's instructions. The fluorescence was quantified via a TECAN microplate reader (TECAN US, Durham, NC).

## 2.7 | In vivo tumor growth and angiogenesis assay

PC3 cells ( $1.5 \times 10^6$ ) with or without pretreatment with G5-FI-RGD-rapamycin (200 nM) for 12 h, were implanted in the flank of SCID mice. Subsequently, human or mouse fibroblasts ( $1.5 \times 10^6$ ) with/without pretreatment with G5-FI-RGD-rapamycin (200 nM) for 12 h were co-implanted with PC3 cells. Tumor volume was calculated twice a week for the duration of the experiment using the formula: Volume ( $\text{mm}^3$ ) = length  $\times$  (width)<sup>2</sup>/2.

After 3 weeks, mice were euthanized and tumors were harvested, fixed, and processed for standard immunohistochemistry. Histological sections were incubated in antigen retrieval solution for 30 min at 90°C, followed by incubation with polyclonal anti-human factor VIII antibody (Lab Vision, Fremont, CA) over night at 4°C.<sup>35</sup> The number of blood vessels in six random fields was counted per experimental condition under light microscope. The care and treatment of experimental animals was in accordance with University of Michigan institutional guidelines. At least three independent experiments were performed to verify reproducibility of results.

## 2.8 | In vivo metastasis assay

PC3 cells that were stably transfected with luciferase (PC3<sup>luc</sup>) cells were injected into the left cardiac ventricle of SCID mice. Four experimental groups were established; group one received 1 mg/kg G5-FI-RGD-rapamycin treatment 48 h before inoculation with tumor cells, group two received treatment at the time of tumor cell inoculation, group three received treatment 48 h after tumor cell inoculation and group four was inoculated with tumor cells and afterwards untreated. G5-FI-RGD-rapamycin was intraperitoneally treated two times per week for 4 weeks. At 1, 2, 3, and 4 week time points, bioluminescence imaging was performed to follow prostate cancer-derived bone metastases as a primary outcome. Immediately prior to each imaging session, the mice were injected intraperitoneally with luciferin (100  $\mu$ L at 40 mg/mL in PBS). Mice were then anesthetized with 1.5% isoflurane/air, using the Xenogen IVIS (Caliper Life Science, Hopkinton, MA) cryogenically cooled imaging system. Bioluminescence generated by the luciferin/luciferase reaction was used for quantification of cancer growth using the LivingImage software (Caliper Life Science). Signal intensity was quantified as the sum of all detected photons during a 1-min luminescent integration time.

## 2.9 | Statistical analyses

Results are presented as mean  $\pm$  standard deviation (SD) or standard error (SE) of mean. Significance of the difference between two measurements was determined by unpaired the Student's *t*-test, and multiple comparisons were evaluated by the Newman-Keuls multiple comparison test. Values of  $P < 0.05$  were considered significant.

# 3 | RESULTS

## 3.1 | Synthesis of G5-FI-RGD-rapamycin dendrimer

To eliminate non-specific binding, generation 5 (G5) dendrimers were partially surface modified with acetic

anhydride (75) and subsequently conjugated with fluorescein isothiocyanate (FI), RGD, and rapamycin (Figure 1A). Gel-permeation chromatography (GPC) was used to confirm dendrimer conjugate homogeneity (Figure 1B). Data generated via a GPC eluogram demonstrated a monodispersed conjugate population with a poly-dispersity index (PDI) of 1.04. To demonstrate that G5 dendrimers functionalized with RGD and rapamycin bind to human bone marrow-derived fibroblasts, the cells were treated with 200 nM G5-FI-RGD-rapamycin for 6 h. Confocal microscopy analysis revealed robust binding and internalization of the conjugate after treatment with 200 nM G5-FI-RGD-rapamycin (Figure 1C). The observed binding was

inhibited when the cells were pre-incubated with 1  $\mu$ M of free RGD peptide for 30 min prior to G5-FI-RGD-rapamycin treatments, confirming specificity (Figure 1C). Flow cytometry analysis confirmed dendrimer binding to fibroblasts as indicated by an increase in fluorescent intensity relative to untreated fibroblasts (Figure 1D). The binding was also blocked when the fibroblasts were pre-incubated with 1  $\mu$ M of free RGD peptide for 30 min prior to G5-FI-RGD-rapamycin treatments (Figure 1D). Together, these results strongly indicate the successful conjugation of a multifunctional G5-FI-RGD-rapamycin dendrimer that specifically targeted cells that express integrin  $\alpha$ V $\beta$ 3.

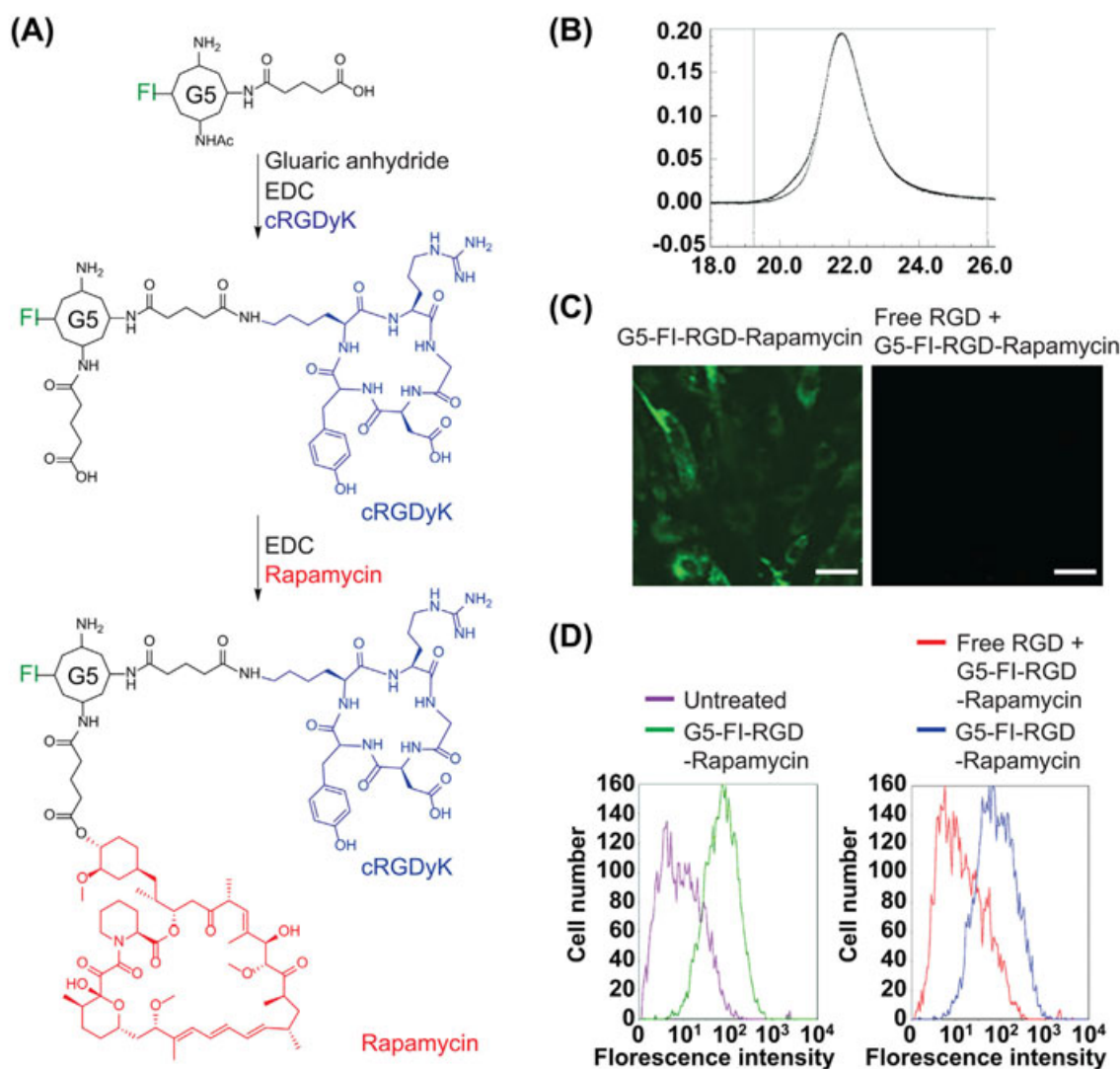


**FIGURE 1** Synthetic scheme and characterization of G5-FI-RGD-rapamycin. A, Synthetic scheme. B, Dendrimer homogeneity was confirmed via GPC with a poly-dispersity index of 1.04. C, Human fibroblasts (HFs) were treated with 200 nM G5-FI-RGD-rapamycin for 6 h. Confocal images. Robust binding was observed after 6 h (left panel) and eliminated by pre-incubation with 1  $\mu$ M free RGD peptide (right panel). Scale bars, 50  $\mu$ m. D, Conjugate binding to HFs was confirmed via flow cytometry (left panel) and eliminated by pre-incubation with 1  $\mu$ M free RGD peptide (right panel)

### 3.2 | G5-FI-RGD-rapamycin inhibits mTOR signaling in fibroblasts and cancer cells

Rapamycin alters protein translation by inhibiting mammalian target of rapamycin complex 1 (mTORC1) signaling.<sup>36–38</sup> Therefore, G5-FI-RGD-rapamycin was tested as an mTORC1 inhibitor. Western blot analysis revealed that treatment with G5-FI-RGD-rapamycin (0.5, 1, 10, or 50 nM) blocked mTORC1-mediated S6K1 phosphorylation (Thr389) at levels similar to free rapamycin treatments in human fibroblasts (Figure 2A). G5-FI-RGD-rapamycin (20 and 200 nM) also strongly inhibited S6K1-mediated phosphorylation of ribosomal protein S6 (rpS6) at levels similar to free rapamycin treatments in HeLa (cervical cancer), PC3 (prostate cancer), and MDA-MB-231 (breast cancer) cells in normal culture

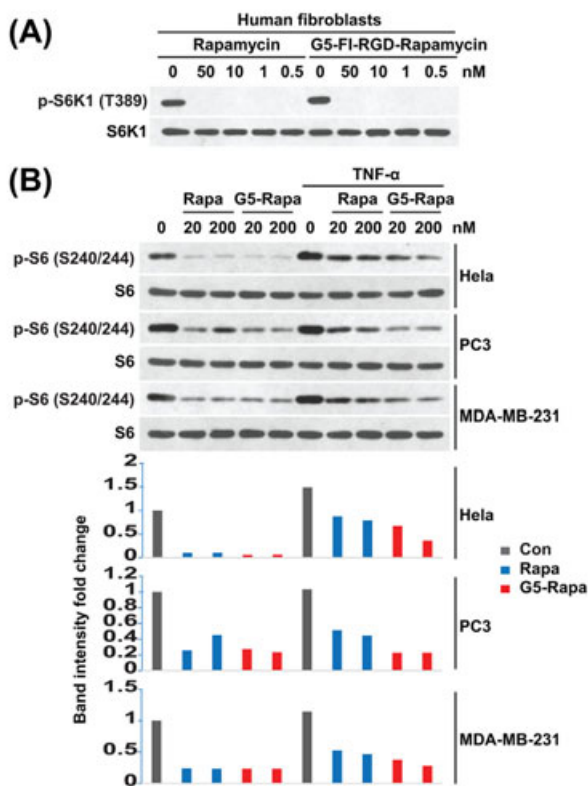


**FIGURE 2** G5-FI-RGD-rapamycin inhibits mTOR signaling in fibroblasts and cancer cells. A, G5-FI-RGD-rapamycin blocked S6K1 phosphorylation at similar levels to free rapamycin treatment. Human fibroblasts were treated with the indicated concentration of free rapamycin or G5-FI-RGD-rapamycin for 24 h and analyzed by Western blotting with the indicated antibodies. B, G5-FI-RGD-rapamycin renders cancer cells sensitive to rapamycin-mediated inhibition of rpS6 phosphorylation under proinflammatory condition. Human cancer cells were treated with the indicated concentration of free rapamycin (Rapa) or G5-FI-RGD-rapamycin (G5-Rapa) with/without TNF- $\alpha$  (20 ng/mL) for 24 h and analyzed by Western blotting with the indicated antibodies. Band intensity for rpS6 phosphorylation was quantified using Image J software and normalized to rpS6

conditions (Figure 2B). Interestingly, when cancer cells were stimulated with TNF- $\alpha$  to mimic proinflammatory conditions, the sensitivity to free rapamycin (both 20 and 200 nM) was significantly reduced (Figure 2B). Critically, in TNF- $\alpha$  stimulated PC3 cells treated with 20 or 200 nM G5-FI-RGD-rapamycin and in TNF- $\alpha$  stimulated HeLa and MDA-MB-231 cells treated with 200 nM G5-FI-RGD-rapamycin, sensitivity to rapamycin was sustained (Figure 2B). These results suggest that G5-FI-RGD-rapamycin significantly inhibits mTOR signaling in cancer cells under proinflammatory conditions more efficiently than unconjugated rapamycin.

### 3.3 | G5-FI-RGD-rapamycin reduces VEGF expression in rapamycin sensitive cells

Growing evidence demonstrates that two key regulators of angiogenesis, vascular endothelial growth factor (VEGF), and fibroblast growth factor (FGF) are up-regulated in both advanced tumor cells and their reactive stromal fibroblast cells.<sup>39–41</sup> To determine how VEGF and FGF-2 expression from cancer cells or fibroblasts respond to G5-FI-RGD-rapamycin, rapamycin sensitive cells (PC3, C42B, and human fibroblast) and rapamycin insensitive cells (HDMEC, MDA-MB-231, and HeLa)<sup>42</sup> were treated with 200 nM G5-FI-RGD-rapamycin for 24 h and VEGF and FGF-2 expression was analyzed by Western blotting. Under these conditions, G5-FI-RGD-rapamycin inhibited VEGF expression in rapamycin-sensitive prostate cancer cells, PC3, C4-2B, and human fibroblast cells (Figure 3A), but there was no impact on rapamycin-insensitive cells, HDMEC, MDA-MB-231, and HeLa cells (Figure 3B). Distinctively, FGF2 expression was not altered by G5-FI-RGD-rapamycin in both rapamycin sensitive cells (Figure 3A) and rapamycin-insensitive cells (Figure 3B).

To investigate the effects of prostate cancer cell-secreted factors on VEGF secretion in human fibroblasts, cells were cultured for 24 h with conditioned medium from PC3 or G5-FI-RGD-rapamycin (200 nM) treated PC3 and analyzed by Western blotting for detection of VEGF and FGF2. Results demonstrated that treatment with conditioned medium from PC3 cells increased VEGF protein levels from human fibroblasts and that conditioned medium from G5-FI-RGD-rapamycin treated PC3 did not increase VEGF protein levels from human fibroblasts (Figure 3C). HDMEC and human or mouse fibroblast cells were treated with 200 nM G5-FL-RGD-rapamycin for 24 h and culture supernatants were assayed by ELISA for detection of secreted VEGF. Results indicated a 50% reduction in VEGF secretion from both human and mouse fibroblasts following G5-FI-RGD-rapamycin treatment (Figure 3D). Taken together, these results suggest that VEGF secretion from fibroblasts is influenced by tumor-secreted factors and that G5-FI-RGD-rapamycin treatment inhibits this effect.

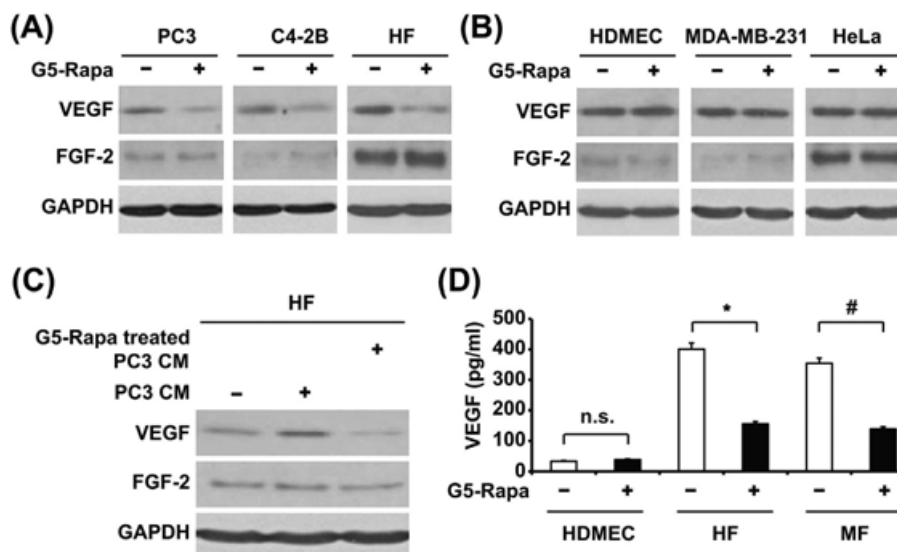


**FIGURE 3** G5-FI-RGD-rapamycin reduces VEGF expression in rapamycin sensitive cells. A, Rapamycin sensitive cells (PC3, C42B, and human fibroblasts [HF]) and (B) rapamycin insensitive cells (HDMEC, MDA-MB-231, and HeLa) were treated with 200 nM G5-FI-RGD-rapamycin (G5-Rapa) for 24 h and analyzed by Western blotting for detection of VEGF and FGF-2 expression. C, HF cells were cultured for 24 h with conditioned medium (CM) from PC3 or G5-FI-RGD-rapamycin (G5-Rapa, 200 nM) treated PC3 and analyzed by Western blotting for detection of VEGF and FGF-2. D, HDMEC and human or mouse fibroblast cells (HF or MF) were treated with G5-FL-RGD-rapamycin (G5-Rapa, 200 nM) for 24 h and culture supernatants were assayed by ELISA for detection of secreted VEGF. Data represent average mean  $\pm$  SD from duplicate assays, and the experiments were performed twice. \* $P < 0.001$ ; # $P < 0.002$ ; n.s., not significant

### 3.4 | G5-RGD-rapamycin inhibits fibroblast mediated PCa progression in vivo

Next, we determined how fibroblasts play a role in tumor progression in vivo, and the extent to which this role is dependent of mTOR signaling. PC3 cells were pretreated with or without 200 nM G5-FI-RGD-rapamycin for 12 h and were injected with either human or mouse fibroblasts into the flanks of SCID mice. In parallel experiments, human or mouse fibroblasts were pre-treated with 200 nM G5-RGD-rapamycin for 12 h prior to co-implantation with PC3 cells. The volume of these tumor xenografts was monitored for 22 days. Treating PC3 cells with 200 nM G5-FL-RGD-rapamycin did not affect tumor progression when compared to PC3 without treatment (Figure 4A). PC3 cells co-implanted with either human or mouse fibroblasts demonstrated a fourfold increase in tumor growth compared to PC3 cells alone (Figure 4A). Pre-treating either the human or mouse fibroblasts with G5-FI-RGD-rapamycin prior to co-implantation did not affect the viability of fibroblasts but reduced fibroblast-mediated tumor growth twofold (Figure 4A). These results suggest that fibroblasts enhance tumor progression and indicate that this enhancement is mTOR signaling dependent.

Because enhanced capillary density is a hallmark of tissue stroma reacting to and promoting tumor progression toward metastasis,<sup>11,23,24</sup> we analyzed the effects of treatment with

G5-FL-RGD-rapamycin on blood vessel density in tumor xenografts in SCID mice. Xenografts from PC3 cells with or without co-implantation with fibroblasts were collected, sectioned, and stained for factor VIII, an essential clotting factor found in blood vessels. In parallel experiments, xenografts from tumors formed from PC3 cells co-implanted with fibroblasts pre-treated with G5-FL-RGD-rapamycin (200 nM) were also sectioned and stained for factor VIII. Blood vessel density of these samples as subsequently quantified. Results revealed that co-implanting PC3 cells with human or mouse fibroblasts increases blood vessel density showing both increased size and number of blood vessels (Figures 4B and 4C). The density was significantly reduced when fibroblasts were treated with G5-FL-RGD-rapamycin before implantation (Figures 4B and 4C).

### 3.5 | G5-RGD-rapamycin inhibits PCa metastasis in vivo

We extended our in vivo studies to include G5-FI-RGD-rapamycin. Luciferase tagged PC3 cells were injected into the left ventricle of the hearts of SCID mice. These mice were then treated with 1 mg/kg G5-FL-RGD-rapamycin under one of the following conditions: Group 1 served as a control in which the animals were untreated to the PC3 cell injections. Group 2 animals were treated with the G5 conjugates 48 h prior to the PC3 cell injections. Group 3 animals were treated

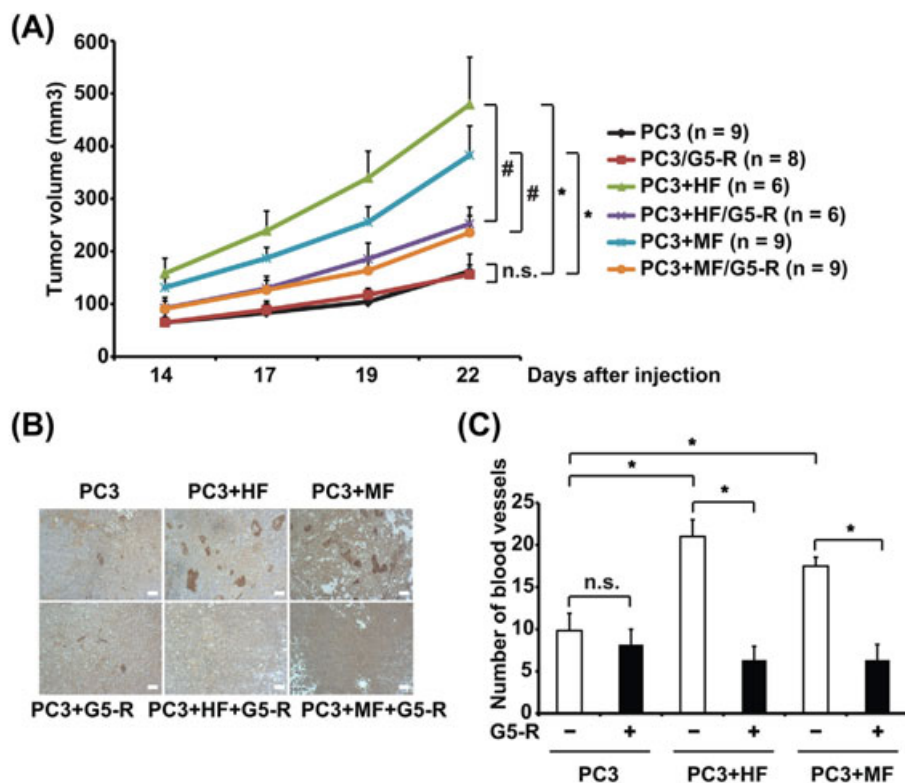


**FIGURE 4** G5-RGD-rapamycin inhibits fibroblast mediated PCa progression in vivo. PC3 cells treated with/without G5-FI-RGD-rapamycin (G5-R, 200 nM) for 12 h were injected or co-injected with either human or mouse fibroblast cells (HF or MF) treated with/without G5-FI-RGD-rapamycin (G5-R, 200 nM) for 12 h into the flank of SCID mice. A, The volume of tumor xenografts was monitored for 22 days. Data represent average mean  $\pm$  SE. \* $P < 0.005$ ; # $P < 0.05$ ; n.s., not significant. The number of mice analyzed is indicated. B, Representative micrographs of factor VIII stained tumor sections at 10X magnification. Scale bars, 200  $\mu$ m. C, The number of blood vessels in six random fields was counted per experimental condition under light microscopy. Data represent average mean  $\pm$  SD. \* $P < 0.001$ ; n.s., not significant

with the G5 conjugates at the time of PC3 cell injections. Group 4 animals were treated with the G5 conjugates 48 h after PC3 cell injections. Thereafter, the G5-FI-RGD-rapamycin was intraperitoneally administered two times per week for 4 weeks in groups 2, 3, and 4. Results were compared to controls that were injected with PC3 cells but not treated with G5 conjugates. Bioluminescence data showed that treatment with G5-FI-RGD-rapamycin significantly reduced tumor burden in the post-treatment group (Group 4) and dramatically reduced tumor burden in the pre-treatment group (Group 2) and immediate-treatment group (Group 3) compared to controls (Group 1) (Figure 5). Taken together, these data suggest G5-FI-RGD-rapamycin is effective in modulating prostate tumor progression and metastasis.

## 4 | DISCUSSION

Groundbreaking research using dendritic nano-polymers for the targeted delivery of therapeutic drugs has demonstrated promising therapeutic potential. Dendritic polymers are currently being evaluated for many in vivo biological

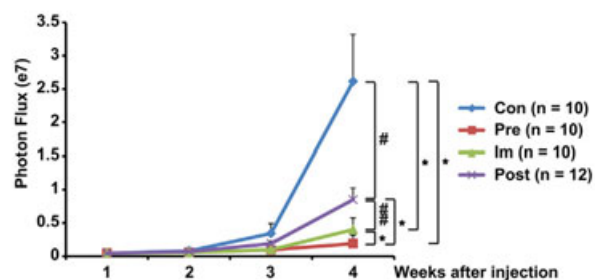


**FIGURE 5** G5-RGD-rapamycin inhibits PCa metastasis in vivo. PC3<sup>luc</sup> cells were injected into the left cardiac ventricle of SCID mice. Experimental groups for G5-FI-RGD-rapamycin treatment (1 mg/kg) were as follows; Con: untreated after PC3<sup>luc</sup> cell inoculation, Pre: 48 h before PC3<sup>luc</sup> cell inoculation, Im: at the time of PC3<sup>luc</sup> cell inoculation, Post: 48 h after PC3<sup>luc</sup> cell inoculation. G5-FI-RGD-rapamycin was intraperitoneally treated two times per week for 4 weeks in Pre, Im, and Post. At 1, 2, 3, and 4 week time points, bioluminescence imaging was performed. Data represent average mean  $\pm$  SD. \* $P < 0.01$ ; # $P < 0.02$ ; ## $P = 0.05$ . The number of mice analyzed is indicated

applications including scaffolds used in tissue engineering, imaging (magnetic resonance, near-infrared, and positron emission), boron-neutron capture therapy, and cancer therapy<sup>43–46</sup> and several first generation nano-carriers are now approved by the FDA.<sup>47–49</sup> However, the development of dendritic polymers that target fibroblasts is just now emerging. Furthermore, using these polymers to modify specific cellular and molecular mechanisms by which fibroblasts modify the microenvironment and enhance tumor metastasis is only beginning to materialize.

In a recent study, investigators described a novel type of fibroblast activation in response to a growing tumor that led to an increased production of growth factors and pro-inflammatory and proteolytic proteins, while at the same time cytoskeletal proteins were degraded.<sup>50</sup> VEGF, HGF/SF, and FGF7 mRNA levels were upregulated to variable degrees in tumor-activated fibroblasts. These activated cells caused an increase in colony unit formation of primary tumor cell lines (UT-SCC-43A and UT-SCC-74A). These results shed light on a study that suggested that human prostatic carcinoma-associated fibroblasts grown with initiated human prostatic epithelial cells dramatically stimulated growth and altered histology of the epithelial population.<sup>51</sup> In addition, they are consistent with our results, which demonstrate that accessory fibroblasts are necessary for prostate tumor progression. We observed that co-implantation of PC3 cells with human fibroblasts exhibited a fourfold increase in tumor volume as compared to PC3 cells alone. In addition, treating these fibroblasts with G5-FI-RGD-rapamycin prior to implantation resulted in a twofold reduction in tumor volume and a marked reduction of blood vessel density in tumors. Together, these data support published reports suggesting that fibroblasts play an important role in tumor progression and further indicate that mTOR signaling may play an important role. Our analysis of two cytokines, VEGF and FGF2, known to play a role in fibroblast-mediated tumor progression revealed that only VEGF is upregulated in fibroblasts by conditioned medium from cancer cells and this increase is eliminated by G5-FI-RGD-rapamycin. Recent studies showed that insulin-like growth factor 2 (IGF2) secreted from cancer cells increases VEGF secretion from cancer-associated fibroblasts.<sup>52</sup> and that mTOR promotes IGF2 expression.<sup>53,54</sup> Thus, IGF2 in PC3 conditioned medium may induce VEGF expression from fibroblasts and IGF2 secretion from PC3 cancer cells may be inhibited by G5-FI-RGD-rapamycin. Inflammatory cytokines such as TNF $\alpha$  activate mTOR signaling and promote tumor angiogenesis via VEGF production.<sup>55</sup> In addition, TNF $\alpha$  increases  $\alpha$ V $\beta$ 3 integrin expression and migration in human cancer cells.<sup>56</sup> Because  $\alpha$ V $\beta$ 3 integrin signaling activates mTOR signaling,<sup>57</sup> it is possible that G5-FI-RGD-rapamycin inhibits mTOR signaling more efficiently than free rapamycin by targeting  $\alpha$ V $\beta$ 3 under inflammatory condition. Indeed, further analysis showed that unlike free rapamycin, G5-FI-

RGD-rapamycin retains its mTOR signaling inhibitory effects in the presence of TNF $\alpha$ . In vivo results confirmed in vitro data by showing that treatment with G5-FI-RGD-rapamycin reduces tumor burden and metastasis in a mouse model. Interestingly, published reports of free rapamycin treatment for this model do not reflect the efficacy we observed in reduction of tumor burden leading us to suspect that there is a dendrimer effect in the observed results. Further investigations are required to determine what mechanisms are responsible for these observations and the results should have important implications for the development of therapies for the treatment of metastatic prostate cancers.

## ACKNOWLEDGMENTS

We thank Dr Yonghyun Lee for the artwork. The work was supported by the National Cancer Institute (CA093900, CA163124), the Department of Defense (W81XW-15-1-0413, W81XWH-14-1-0403), and the Prostate Cancer Foundation.

## CONFLICTS OF INTEREST

The authors have no potential conflicts of interest.

## ORCID

Jin Koo Kim  <http://orcid.org/0000-0003-4268-1118>

## REFERENCES

- Sporn MB. The war on cancer. *Lancet*. 1996;347:1377–1381.
- Tse JC, Kalluri R. Mechanisms of metastasis: epithelial-to-mesenchymal transition and contribution of tumor microenvironment. *J Cell Biochem*. 2007;101:816–829.
- Bhowmick NA, Neilson EG, Moses HL. Stromal fibroblasts in cancer initiation and progression. *Nature*. 2004;432:332–337.
- Canon JR, Roudier M, Bryant R, et al. Inhibition of RANKL blocks skeletal tumor progression and improves survival in a mouse model of breast cancer bone metastasis. *Clin Exp Metastasis*. 2008;25:119–129.
- Bussard KM, Gay CV, Mastro AM. The bone microenvironment in metastasis; what is special about bone? *Cancer Metastasis Rev*. 2008;27:41–55.
- Doehn U, Hauge C, Frank SR, et al. RSK is a principal effector of the RAS-ERK pathway for eliciting a coordinate promotile/invasive gene program and phenotype in epithelial cells. *Mol Cell*. 2009;35:511–522.
- Dai Y, Xu C, Sun X, Chen X. Nanoparticle design strategies for enhanced anticancer therapy by exploiting the tumour microenvironment. *Chem Soc Rev*. 2017;46:3830–3852.
- Folkman J. The role of angiogenesis in tumor growth. *Semin Cancer Biol*. 1992;3:65–71.
- Weidner N, Folkman J, Pozza F, et al. Tumor angiogenesis: a new significant and independent prognostic indicator in early-stage breast carcinoma. *J Natl Cancer Inst*. 1992;84:1875–1887.



10. Dai J, Kitagawa Y, Zhang J, et al. Vascular endothelial growth factor contributes to the prostate cancer-induced osteoblast differentiation mediated by bone morphogenetic protein. *Cancer Res.* 2004;64:994–999.
11. Kaplan RN, Riba RD, Zacharoulis S, et al. VEGFR1-positive haematopoietic bone marrow progenitors initiate the pre-metastatic niche. *Nature.* 2005;438:820–827.
12. Liotta LA, Kohn EC. The microenvironment of the tumour-host interface. *Nature.* 2001;411:375–379.
13. Hattori K, Heissig B, Wu Y, et al. Placental growth factor reconstitutes hematopoiesis by recruiting VEGFR1(+) stem cells from bone-marrow microenvironment. *Nat Med.* 2002;8:841–849.
14. Decaussin M, Sartelet H, Robert C, et al. Expression of vascular endothelial growth factor (VEGF) and its two receptors (VEGF-R1-Flt1 and VEGF-R2-Flk1/KDR) in non-small cell lung carcinomas (NSCLCs): correlation with angiogenesis and survival. *J Pathol.* 1999;188:369–377.
15. Kuhn H, Hammerschmidt S, Wirtz H. Targeting tumorangiogenesis in lung cancer by suppression of VEGF and its receptor—results from clinical trials and novel experimental approaches. *Curr Med Chem.* 2007;14:3157–3165.
16. Ito TK, Ishii G, Chiba H, Ochiai A. The VEGF angiogenic switch of fibroblasts is regulated by MMP-7 from cancer cells. *Oncogene.* 2007;26:7194–7203.
17. Yang F, Strand DW, Rowley DR. Fibroblast growth factor-2 mediates transforming growth factor-beta action in prostate cancer reactive stroma. *Oncogene.* 2008;27:450–459.
18. Gleave M, Hsieh JT, Gao CA, von Eschenbach AC, Chung LW. Acceleration of human prostate cancer growth in vivo by factors produced by prostate and bone fibroblasts. *Cancer Res.* 1991;51:3753–3761.
19. Hwang RF, Moore T, Arumugam T, et al. Cancer-associated stromal fibroblasts promote pancreatic tumor progression. *Cancer Res.* 2008;68:918–926.
20. Pollard JW. Macrophages define the invasive microenvironment in breast cancer. *J Leukoc Biol.* 2008;84:623–630.
21. Tuxhorn JA, McAlhany SJ, Dang TD, Ayala GE, Rowley DR. Stromal cells promote angiogenesis and growth of human prostate tumors in a differential reactive stroma (DRS) xenograft model. *Cancer Res.* 2002;62:3298–3307.
22. Orimo A, Gupta PB, Sgroi DC, et al. Stromal fibroblasts present in invasive human breast carcinomas promote tumor growth and angiogenesis through elevated SDF-1/CXCL12 secretion. *Cell.* 2005;121:335–348.
23. Kalluri R, Zeisberg M. Fibroblasts in cancer. *Nat Rev Cancer.* 2006;6:392–401.
24. Zeisberg EM, Potenta S, Xie L, Zeisberg M, Kalluri R. Discovery of endothelial to mesenchymal transition as a source for carcinoma-associated fibroblasts. *Cancer Res.* 2007;67:10123–10128.
25. Scaffidi AK, Moodley YP, Weichselbaum M, Thompson PJ, Knight DA. Regulation of human lung fibroblast phenotype and function by vitronectin and vitronectin integrins. *J Cell Sci.* 2001;114:3507–3516.
26. Laplante M, Sabatini DM. MTOR signaling in growth control and disease. *Cell.* 2012;149:274–293.
27. Villa-Diaz LG, Kim JK, Laperle A, Palecek SP, Krebsbach PH. Inhibition of FAK signaling by integrin alpha6beta1 supports human pluripotent stem cell self-renewal. *Stem Cells.* 2016;34:1753–1764.
28. Krebsbach PH, Villa-Diaz LG. The role of integrin alpha6 (CD49f) in stem cells: more than a conserved biomarker. *Stem Cells Dev.* 2017;26:1090–1099.
29. Hynes RO. Integrins: bidirectional, allosteric signaling machines. *Cell.* 2002;110:673–687.
30. Kwakwa KA, Sterling JA. Integrin alphavbeta3 signaling in tumor-Induced bone disease. *Cancers (Basel).* 2017;9:84.
31. Hill E, Shukla R, Park SS, Baker JR, Jr. Synthetic PAMAM-RGD conjugates target and bind to odontoblast-like MDPC 23 cells and the predentin in tooth organ cultures. *Bioconjug Chem.* 2007;18:1756–1762.
32. Rameshwar Shukla EH, Shi X, Kim J, Muniz MC, Sun K, Baker RJ, Jr. Tumor microvasculature targeting with dendrimer-entrapped gold nanoparticles. *Soft Matter.* 2008;4:2160–2163.
33. Wang J, Ying G, Wang J, et al. Characterization of phosphoglycerate kinase-1 expression of stromal cells derived from tumor microenvironment in prostate cancer progression. *Cancer Res.* 2010;70:471–480.
34. Jung Y, Kim JK, Shiozawa Y, et al. Recruitment of mesenchymal stem cells into prostate tumours promotes metastasis. *Nat Commun.* 2013;4:1795.
35. Nor JE, Christensen J, Mooney DJ, Polverini PJ. Vascular endothelial growth factor (VEGF)-mediated angiogenesis is associated with enhanced endothelial cell survival and induction of Bcl-2 expression. *Am J Pathol.* 1999;154:375–384.
36. Schmelzle T, Hall MN. TOR, a central controller of cell growth. *Cell.* 2000;103:253–262.
37. Martin DE, Soulard A, Hall MN. TOR regulates ribosomal protein gene expression via PKA and the Forkhead transcription factor FHL1. *Cell.* 2004;119:969–979.
38. Guertin DA, Sabatini DM. Defining the role of mTOR in cancer. *Cancer Cell.* 2007;12:9–22.
39. Ferrara N, Kerbel RS. Angiogenesis as a therapeutic target. *Nature.* 2005;438:967–974.
40. Fukumura D, Xavier R, Sugiura T, et al. Tumor induction of VEGF promoter activity in stromal cells. *Cell.* 1998;94:715–725.
41. Nor JE, Polverini PJ. Role of endothelial cell survival and death signals in angiogenesis. *Angiogenesis.* 1999;3:101–116.
42. Sarbasov DD, Ali SM, Sengupta S, et al. Prolonged rapamycin treatment inhibits mTORC2 assembly and Akt/PKB. *Mol Cell.* 2006;22:159–168.
43. Lee CC, MacKay JA, Frechet JM, Szoka FC. Designing dendrimers for biological applications. *Nat Biotechnol.* 2005;23:1517–1526.
44. Paleos CM, Tsiourvas D, Sideratou Z. Molecular engineering of dendritic polymers and their application as drug and gene delivery systems. *Mol Pharm.* 2007;4:169–188.
45. Tomalia DA, Reyna LA, Swenson S. Dendrimers as multi-purpose nanodevices for oncology drug delivery and diagnostic imaging. *Biochem Soc Trans.* 2007;35:61–67.
46. Pan D, She W, Guo C, Luo K, Yi Q, Gu Z. PEGylated dendritic diamincyclohexyl-platinum (II) conjugates as pH-responsive drug delivery vehicles with enhanced tumor accumulation and antitumor efficacy. *Biomaterials.* 2014;35:10080–10092.
47. Ellerhorst JA, Bedikian A, Ring S, Buzaid AC, Eton O, Legha SS. Phase II trial of doxil for patients with metastatic melanoma refractory to frontline therapy. *Oncol Rep.* 1999;6:1097–1099.
48. Fassas A, Anagnostopoulos A. The use of liposomal daunorubicin (DaunoXome) in acute myeloid leukemia. *Leuk Lymphoma.* 2005;46:795–802.

49. Green MR, Manikhas GM, Orlov S, et al. Abraxane, a novel Cremophor-free, albumin-bound particle form of paclitaxel for the treatment of advanced non-small-cell lung cancer. *Ann Oncol*. 2006;17:1263–1268.
50. Rasanen K, Virtanen I, Salmenpera P, Grenman R, Vaheri A. Differences in the chemotaxis response of normal and cancer-associated fibroblasts from patients with oral squamous cell carcinoma. *PLoS ONE*. 2009;4:e6879.
51. Olumi AF, Grossfeld GD, Hayward SW, Carroll PR, Tlsty TD, Cunha GR. Carcinoma-associated fibroblasts direct tumor progression of initiated human prostatic epithelium. *Cancer Res*. 1999;59:5002–5011.
52. Xu WW, Li B, Guan XY, et al. Cancer cell-secreted IGF2 instigates fibroblasts and bone marrow-derived vascular progenitor cells to promote cancer progression. *Nat Commun*. 2017;8:14399.
53. Dai N, Rapley J, Angel M, Yanik MF, Blower MD, Avruch J. mTOR phosphorylates IMP2 to promote IGF2 mRNA translation by internal ribosomal entry. *Genes Dev*. 2011;25:1159–1172.
54. Dai N, Christiansen J, Nielsen FC, Avruch J. mTOR complex 2 phosphorylates IMP1 cotranslationally to promote IGF2 production and the proliferation of mouse embryonic fibroblasts. *Genes Dev*. 2013;27:301–312.
55. Lee DF, Kuo HP, Chen CT, et al. IKK beta suppression of TSC1 links inflammation and tumor angiogenesis via the mTOR pathway. *Cell*. 2007;130:440–455.
56. Hou CH, Yang RS, Hou SM, Tang CH. TNF-alpha increases alpha5beta1 integrin expression and migration in human chondrosarcoma cells. *J Cell Physiol*. 2011;226:792–799.
57. Lee DY, Li YS, Chang SF, et al. Oscillatory flow-induced proliferation of osteoblast-like cells is mediated by alpha5beta1 and beta1 integrins through synergistic interactions of focal adhesion kinase and Shc with phosphatidylinositol 3-kinase and the Akt/mTOR/p70S6K pathway. *J Biol Chem*. 2010;285:30–42.

**How to cite this article:** Hill EE, Kim JK, Jung Y, et al. Integrin alpha V beta 3 targeted dendrimer-rapamycin conjugate reduces fibroblast-mediated prostate tumor progression and metastasis. *J Cell Biochem*. 2018;119:8074–8083.  
<https://doi.org/10.1002/jcb.26727>